Pharm Res (2013) 30:32–40
DOI 10.1007/s11095-012-0846-x

RESEARCH PAPER

Effect of Vehicles on the Maximum Transepidermal Flux of Similar Size Phenolic Compounds

Qian Zhang • Peng Li • David Liu • Michael S. Roberts

Received: 23 May 2012 / Accepted: 30 July 2012 / Published online: 25 August 2012

ABSTRACT

Purpose In principle, maximum transepidermal fluxes of solutes should be similar for different vehicles, except when the solute or vehicle modifies the skin. Here we estimated maximum flux, stratum corneum solubility, diffusivity and permeability coefficient for a range of similarly sized phenolic compounds with varying lipophilicity from polar and lipophilic vehicles.

Methods Maximum flux and other skin transport parameters through human epidermis were obtained from lipophilic vehicles (mineral oil (MO) and isopropyl myristate (IPM)) and compared with values from water and propylene glycol (PG)-water solutions. Solvent uptake and changes in stratum corneum infrared spectroscopy and multiphoton microscopy imaging were also investigated.

Results Maximum fluxes for MO and water were similar but IPM has a higher value for more polar phenols due to a higher diffusivity and PG-water had a higher flux due to higher solubility in the stratum corneum. Whereas maximum flux for various phenols was directly related to solubility in the stratum corneum independent of vehicle, increasing phenol lipophilicity increased and decreased permeability coefficient for aqueous solvents and lipophilic solvents, respectively.

Conclusion The maximum fluxes for phenols with a similar molecular size and varying lipophilicity were comparable between water and MO vehicles but higher for IPM and PG-water mixtures.

Q. Zhang • P. Li • M. S. Roberts
School of Pharmacy and Medical Sciences
University of South Australia
Adelaide, SA 5001, Australia

D. Liu • M. S. Roberts (✉)
Therapeutics Research Centre, School of Medicine
University of Queensland, Princess Alexandra Hospital
Woolloongabba, QLD 4102, Australia
e-mail: m.roberts@uq.edu.au

KEY WORDS diffusivity · lipophilic vehicle · maximum flux · permeability coefficient · solubility in the stratum corneum

ABBREVIATIONS

ATR-FTIR	attenuated total reflectance Fourier transform infrared
C_v	solute concentration in the vehicle
D^*	diffusivity per unit path length
HPLC	high-performance liquid chromatography
IPM	isopropyl myristate
$J_{max,estimated}$	maximum fluxes estimated from dilute solutions
J_{ss}	steady-state flux
$K_{IPM,\ pool}$	partition coefficient between IPM lipid pool and usual path for solute diffusion in stratum corneum
k_p	permeability coefficient
K_{SC}	stratum corneum-vehicle partition coefficient
log P	logarithmic (base 10) form of octanol-water partition coefficient
MO	mineral oil
PBS	phosphate buffered saline
PG	propylene glycol
Q_{ss}	cumulative amount of solute penetrated at steady state
S_v	solute solubility in the vehicle
S_f	solvent factor
S_{SC}	solute solubility in the stratum corneum
t_{lag}	lag time
W_F	weight fraction

INTRODUCTION

It is generally recognised that, provided a topical formulation does not affect the skin, the maximal and

fractional flux of individual solutes will be the same from all vehicles (1,2). For instance, Twist and Zatz (3) showed that methyl paraben had the same flux across polydimethylsiloxane membrane for a range of different solubilities in various vehicles. Cross *et al.* (4) showed a similar result for hydrocortisone through silicone membranes. Barry *et al.* (5) showed that benzyl alcohol flux was also a function of thermodynamic activity in a vehicle independent manner. Lippold (6) also gave several examples of solutes such as steroids where either flux or therapeutical activity (vasoconstrictor response) was related to thermodynamic activity and not to the nature of the vehicle.

We have shown that molecular size is a major determinant of skin penetration (7) and subsequently showed that similarly sized phenolic compounds when applied to the skin in water have a parabolic relationship between maximum flux and log *P* (logarithmic (base 10) form of octanol-water partitioning coefficient) (8). Many phenols are used clinically as analgesics and as preservatives in various vehicles (9,10). However, there appears to be limited systemic studies examining the effects of these vehicles on the maximum transdermal flux of solutes through the skin, recognising that some vehicles may promote skin penetration (2). We have now shown that polar propylene glycol (PG)-water mixtures enhanced skin penetration through the partitioning of PG into skin lipids resulting in an enhanced solubility of the phenols in stratum lipids (11).

In this work, we expand on previous studies to include the effects of lipophilic vehicles on the maximum flux of a range of phenolic compounds of similar size but different lipophilicity across the human epidermis. We chose the most inert lipophilic vehicle, mineral oil (MO), and the commonly used vegetable oil equivalent, isopropyl myristate (IPM), as our model vehicles. The odourless and lightweight MO, which mainly consists of straight chain saturated hydrocarbons with carbon numbers greater than 20 (12), is as an ideal emollient to mimic the moisturizing function of natural lipids in the stratum corneum by their contribution to water retention (13,14). IPM is also widely found in cosmetic and topical medicinal preparations with a capacity to enhance solute transdermal absorption (15,16).

We measured the transdermal maximum fluxes in Franz cells using human epidermis, in addition, as described previously for water and PG-water vehicles (8,11), we measured the solubility of phenols in the stratum corneum and determined their diffusivity. In order to understand the nature of the vehicle effects on the skin bio-properties, we also used the attenuated total reflectance Fourier transform infrared (ATR-FTIR) spectroscopy and multiphoton microscopy.

MATERIALS AND METHODS

Chemicals

Methyl paraben (99%), β-naphthol (99%), methyl salicylate (99%), chlorocresol (99%), thymol (98%), mineral oil, isopropyl myristate, phosphate buffered saline (PBS) sachets, acetonitrile and ethanol were purchased from Sigma-Aldrich (Castle Hill, NSW, Australia). 4-Propoxyphenol (99%), iso-thymol (99%), o-t-butylphenol (99%), chloroxylenol (99%), and p-n-butylphenol (99%) were supplied by Novachem Pty Ltd (Collingwood, Vic., Australia).

Sample Analysis

Solute concentrations in all samples were analysed by a high-performance liquid chromatography (HPLC) system consisting of a Shimadzu SIL- 6B® SCL-10A VP system controller, a SPD-10AV UV–VIS detector, a LC-10 AD pump and an autoinjector, with a C8 reverse phase column (3.5 μm, 150× 4.6 mm), using previously described methods (8).

Solubility in MO and IPM

The solubility of each test solute in MO and IPM at 32°C was obtained separately from a partitioning experiment due to the impossibility of injecting MO directly into the HPLC system and the fact that it would need huge amount of the compounds to achieve a saturation state in IPM. The method used here is similar to that of measuring octanol-water partitioning coefficient. Three known concentrations (C_v) of one solute in water solution (in 6 mL) were prepared and equilibrated with 4 mL of MO or IPM by continuous mixing at 32°C for 72 h. Samples from the water phase were subsequently obtained and prepared for HPLC analysis. The solubility in the vehicle (S_v) is thereafter calculated by: $S_{MO\ (\text{or } IPM)} = S_{water} \times C_{MO(\text{or } IPM)}/C_{water}$.

Preparation of Isolated Human Epidermis and Stratum Corneum

Human skin samples were obtained from a female patient who had undergone abdominal plastic surgery with ethical approval from the Queen Elizabeth Hospital and the University of South Australia Human Research Ethics Committees. The subcutaneous fatty tissue was removed with a scalpel, and the epidermis separated from the dermis by immersing the skin in water at 60°C for 90 sec (17). The epidermis was stored in polyethylene bags at −20°C. The stratum corneum was obtained by floating the epidermal membranes overnight on a solution of 0.005% trypsin in

PBS (pH 7.4) at 37°C (17). Stratum corneum sheets placed on aluminium foil were stored frozen at −20°C.

Solute Solubility in the Stratum Corneum (S_{SC})

S_{SC} was obtained by partitioning tests. Pre-weighted circles of stratum corneum (1–1.5 mg, 4 replicates for each solute) were soaked in screw-topped glass vials with saturated solutions of each test solute and equilibrated at 32°C for 24 h (18,19). The solute in the stratum corneum was then extracted by immersing the blotted dry stratum corneum into 1 mL of 70% ethanol/water. The solute concentration in the equilibrating solution was measured by HPLC to determine if the solution remained saturated (i.e. a loss < 1%). The S_{SC} was calculated by the amount of the solute recovered in the extraction fluid, divided by the weight of the stratum corneum before equilibration.

In Vitro Penetration Studies

Human epidermal membranes with stratum corneum side up were mounted on vertical Franz-type diffusion cells (exposed surface area about 1.3 cm^2, 4–5 replicates for each solute). A 10% ethanol/PBS buffer, the same used as in previous studies (8), was used as the receptor phase to ensure sink conditions and the results are comparable. The receptor phase was continuously stirred with magnetic stirrer bars and maintained in a water bath at 35°C. Infinite doses (solute concentrations were 10–50% of their saturated concentrations in the vehicle) were applied to the surface and the top of the diffusion cell was covered with a glass cover slip. 200 µL samples of the receptor phase were removed and replaced with fresh solution at set time points over a 24 h period. After the last sampling time, the donor solution was also collected.

Solute steady-state flux (J_{ss}) across the membrane was estimated from the gradient of linear regression plots of the cumulative amount of solute penetrated (Q_{ss}) through the diffusion area (A) against time:

$Q_{ss}(t) = J_{ss}A\left(t - t_{lag}\right)$. Lag time ($t_{lag}$) value corresponds to the t-intercept of the linear steady-state limit. Estimated maximum flux from dilute solutions ($J_{\max,estimated}$) is then obtained by: $J_{\max,estimated} = J_{SS}S_v/C_v$.The apparent diffusivity per unit path length (D^*) can be estimated as: $D^* = J_{\max,estimated}/S_{SC}$. The permeability coefficient (k_p) is estimated as: $k_p = J_{\max,estimated}/S_v$, and the stratum corneum-vehicle partition coefficient (K_{SC}) is calculated as: $K_{SC} = S_{SC}/S_v$.

Swelling of the Stratum Corneum by Solvent Uptake

The uptake of MO and IPM into the stratum corneum was measured by the weight difference (Mettler ME22 microbalance) method by soaking the dry stratum corneum sheets (about 2–3 mg) in 5 mL of the solvent at 32°C respectively. Weight fraction (W_F) [$= W_S/(W_S + W_{SC})$ (mg/mg)] was used as an indicator of swelling degree of the stratum corneum by the solvent uptake, where W_S is the total weight of solvent absorbed in the stratum corneum (i.e. the weight difference) and the W_{SC} is the weight of the dry stratum corneum.

ATR-FTIR Spectroscopic Study

The stratum corneum side of the full thickness skin after equilibrating at 25°C for 1 h was first recorded as a control (with 3 replicates). The skin was then placed (dermis down) on a filter paper soaked with PBS buffer, with a cotton swab soaked in one of the vehicles on top for 12 h at 25°C. The treated skin samples were washed with distilled water and blotted dry. The infrared spectra of skin samples were obtained using Bruker Tensor 27 FTIR spectrometer (Bruker Optik GmbH, Ettlingen, Germany) with a ZnSe reflectance element (PIKE Technologies, Inc. Madison, United States). The spectra were collected in the wavenumber range of 4000–600 cm^{-1} with 16 scans at a resolution of 4 cm^{-1}. Analysis was performed with the OPUS 6.5 program (Bruker Optik GmbH, Ettlingen, Germany).

Tape stripping (D-SQUAME® Stripping Discs D100, CuDerm Corporation, Dallas, TX, United States) was performed to obtain the spectra of deeper layers of the stratum corneum with a purpose to trace any change of the stratum corneum and any penetration of the solvent into the deeper layers by FTIR.

Multiphoton Microscopy Study

The skin samples for microscopy imaging were prepared in a similar manner to as for *in vitro* Franz-cell penetration studies, but instead of using skin epidermis, the unfrozen full thickness skin was used. Saturated solution of fluorescent β-naphthol from water, 40%PG/water, MO and IPM were added to the donor chamber (i.e. the stratum corneum side) and left for 12 h before image collection. Control samples were prepared by using the vehicle only on the stratum corneum side without β-naphthol (20).

The distribution of β-naphthol in the stratum corneum was examined with the Zeiss LSM710 multiphoton microscopy system (Carl Zeiss MicroImaging GmbH, Germany), coupled to a short (85 femtosecond pulse width) pulsed mode-locked 80-MHz Ti: Sapphire MaiTai laser (Spectra Physics, Mountain View, United States) and a Plan-Apochromat 63X/1.40 oil objective lens (Carl Zeiss MicroImaging GmbH, Germany). The multiphoton microscopy imaging of β-naphthol was performed with multiphoton excitation at 736 nm and detector spectral wavelength from 350 to 650 nm.

RESULTS

The penetration data for the 10 phenolic compounds in MO and IPM through excised human epidermis are listed in Tables I and II. Figure 1 shows the maximum values obtained with those we previously reported for water (8). It is evident that that the maximum fluxes obtained for MO are similar to those obtained for water. In both cases, a bilinear convex relationship exists between log $J_{\max,estimated}$ and log P with a highest flux around log P 2.9-3.2. In contrast, the IPM vehicle led to an enhanced penetration of all phenolic compounds and was most marked for the more polar phenols (i.e. those with low log P, Fig. 1). Also included in Fig. 1 are the enhanced maximum flux values we reported previously for 40% PG/water (11).

Table I shows that the experimental solubility data of the phenols in MO is generally lower than in the stratum corneum. In contrast, the solubility of phenols in IPM is much greater than for MO (Table II). As a consequence, the partition coefficient between the stratum corneum and vehicle, $K_{SC,}$ for phenols range from 0.7 to almost 400 for the MO vehicle (Table I) whereas for the IPM vehicle they range from 0.2 up to 1.1 (Table II). Clearly, K_{SC} alone does not predict that the observed maximum fluxes for phenols will be much greater from IPM than from MO (Fig. 1). Further, whereas the maximum fluxes for all phenols show a similar trend with log P for all vehicles (Fig. 1), the slope of the relationships between log K_{SC} and log P is positive for the polar vehicles, water and 40%PG/water, but negative for the lipophilic vehicles, MO and IPM (Fig. 2). Consistent with k_p being defined as $K_{SC}.D^*$, its dominant determinant is K_{SC} and plots of log k_p against log P also show positive slopes for polar vehicles but negative slopes for lipophilic vehicles (Fig. 3).

The two determinants of maximum flux are the solubility of phenols in the stratum corneum (S_{SC}) and its diffusivity adjusted for path length (D^*). It is evident from Fig. 4 that S_{SC} dominates in determining the shape of log $J_{\max,estimated}$ *versus* log P in that, for all vehicles, the plot of log S_{SC} against log P is similar in shape to that described between log $J_{\max,estimated}$ and log P (Fig. 1).

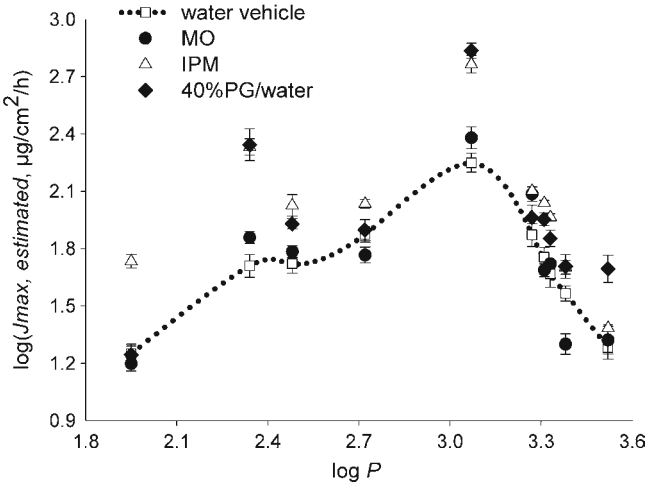

Fig. 1 log $J_{max,\ estimated}$ values from four vehicles *versus* log P (Points represent the mean±SD, the dashed line included is the interpolation of the data for the water vehicle *versus* log P only).

Indeed, when log $J_{\max,estimated}$ is plotted against log S_{SC}, a positive similar slope is evident for MO and IPM (Fig. 5). The differences in the actual slopes are likely to be due in part to the different affinity of the various vehicles for the stratum corneum as the immersion of dry stratum corneum in the various vehicles led to an uptake of 5.3±1.6% for MO, 16.8±4.4% for IPM, 45.1±3.7% for water and 66.4±4.5% for 40%PG/water. Interestingly, whereas there appears to be a single linear relationship for MO as the vehicle (Fig. 5, r^2=0.84), IPM appears to have two components with different slopes, one with a log P of phenols < 3.1

Table I Relevant Physicochemical Parameters and Permeation Data of Phenolic Solutes in MO Through Human Skin: Maximum Fluxes Estimated from Dilute Solutions (log $J_{max,\ estimated}$), The Lag Time (t_{lag}) and the Diffusivity Per Unit Path Length (D^*). The Solute Solubility in the Vehicle (S_v), in the Stratum Corneum (S_{SC}), and the Estimated Partitioning Values (K_{SC}). Values Obtained in this Work are Expressed as mean±SD

Phenolic Compound	MW [a]	log P (exp)	log ($J_{max,\ estimated}$) (µg/cm^2/h)	t_{lag} (h)	log (D^*10) (mg/cm^2/h)	S_v (32°C) (mg/mL)	S_{SC} (32°C) (µg/mg)	K_{SC} (mL/g)
methyl paraben	152	1.95±0.03	1.20±0.04	0.98±0.08	0.88±0.06	0.05±0.00	20.75±0.91	391.10±48.48
4-propoxyphenol	152	2.34±0.06	1.86±0.03	1.08±0.24	1.03±0.07	0.20±0.01	68.03±5.37	340.60±46.89
methyl salicylate	152	2.48±0.05	1.78±0.03	0.71±0.36	1.09±0.13	72.15±10.32	49.16±11.44	0.68±0.26
β−naphthol	144	2.72±0.02	1.77±0.04	0.69±0.24	1.03±0.07	3.06±0.30	53.93±3.47	17.62±2.87
chlorocresol	143	3.07±0.04	2.38±0.06	1.38±0.21	0.96±0.03	24.98±1.87	261.04±11.44	10.45±1.24
iso-thymol	150	3.27±0.03	2.09±0.04	0.96±0.35	1.09±0.11	50.67±4.00	99.90±15.90	1.97±0.47
thymol	150	3.31±0.02	1.69±0.03	1.95±0.25	0.91±0.14	44.57±3.40	60.39±15.07	1.36±0.44
o-t-butylphenol	150	3.33±0.03	1.72±0.01	1.23±0.25	0.98±0.09	43.83±2.33	55.74±9.94	1.27±0.30
chloroxylenol	156	3.38±0.02	1.30±0.05	1.61±0.46	0.91±0.06	0.82±0.07	24.40±2.59	29.68±5.72
p-n-butylphenol	150	3.52±0.03	1.32±0.07	1.09±0.54	0.93±0.12	4.93±0.39	24.61±2.76	5.00±0.95

[a] MW, molecular weight; data from web version of SciFinder

Table II Relevant Physicochemical Parameters, Permeation Data and Solubility Values of Phenolic Solutes in IPM Through Human Skin, Values Obtained in This Work are Expressed as mean±SD

Phenolic Compound	*log* ($J_{max,\ estimated}$) ($\mu g/cm^2/h$)	t_{lag} (h)	*log (D*10)* ($mg/cm^2/h$)	S_v (32°C) (mg/mL)	S_{SC} (32°C) ($\mu g/mg$)	K_{SC} (mL/g)
methyl paraben	1.73±0.04	2.16±0.79	1.18±0.06	31.39±2.19	35.42±2.33	1.13±0.15
4-propoxyphenol	2.33±0.04	2.69±1.61	1.14±0.10	237.53±13.62	155.54±20.61	0.65±0.12
methyl salicylate	2.03±0.06	0.97±0.30	1.14±0.12	385.27±26.68	76.53±11.41	0.20±0.04
β−naphthol	2.03±0.02	3.22±0.70	1.11±0.07	258.36±15.60	83.42±10.38	0.32±0.06
chlorocresol	2.77±0.05	1.91±0.09	1.00±0.06	1513.06±89.06	578.46±47.64	0.38±0.05
iso-thymol	2.10±0.02	2.62±0.51	0.65±0.05	1344.53±102.01	284.96±17.90	0.21±0.03
thymol	2.04±0.01	1.71±0.30	0.63±0.08	1281.80±104.04	258.33±39.07	0.20±0.05
o-t-butylphenol	1.96±0.02	3.18±1.42	0.48±0.05	1746.85±116.32	303.08±21.31	0.17±0.02
chloroxylenol	1.70±0.04	1.85±0.63	0.82±0.09	313.68±22.87	76.96±9.26	0.25±0.05
p-n-butylphenol	1.38±0.02	1.73±0.55	0.55±0.03	271.49±15.85	67.52±2.48	0.25±0.02

(Fig. 5, r^2=0.99) and the second with a log P>3.1 (Fig. 5, r^2=0.85).

The second determinant of maximum flux, D^*, is clearly not determining the shape for MO, water or 40% PG/water, as D^* is almost constant and independent of log P (Fig. 6). In contrast, D^* is higher for the more polar phenols but decreases for the more lipophilic solutes. This decrease in D^* is most marked for phenols with a log P>2.8 (Fig. 6).

An ATR-FTIR examination of IPM in stratum corneum showed the presence of the C-O stretching vibration from the ester group of IPM at 1110 cm^{-1} (Fig. 7), consistent with IPM dissolving in deeper stratum corneum layers. This peak was evident down to the 15th stratum corneum tape strip.

Figure 8 shows the distribution of β-naphthol fluorescence in the human stratum corneum at a depth of 5 μm below the skin surface after 12 h exposure to the saturated solutions from different vehicles (a2–d2) and corresponding vehicle only treated samples as the control (a1–d1). These images demonstrate that the highest concentrations of β-naphthol are located in the intercellular region of the stratum corneum for the polar vehicles, water and PG-water cosolvents. In contrast, there appears to be an increase in the fluorescence for the lipophilic vehicles, MO and IPM in the corneocytes, suggesting that these vehicles enter the corneocytes and increase S_{SC}. Indeed, the boundary between the lipid wall and the cell is less after treatment with IPM (Fig. 8d).

DISCUSSION

This work adds to our mechanistic understanding on how vehicles affect the penetration of different solutes. Importantly, our findings suggest that the relatively inert lipophilic vehicle MO yields similar maximum fluxes to a water vehicle for a series of phenols with log P of 1.95 to 3.52 through excised human skin, but the more semipolar vehicle IPM produces anomalous behaviour in the maximum fluxes dependency on log P for the various phenols studied here.

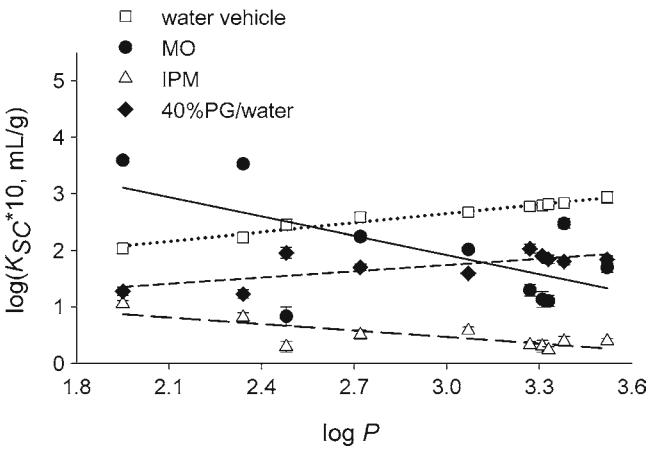

Fig. 2 The plot of log K_{SC} *versus* log *P* (the lines show the linear fit).

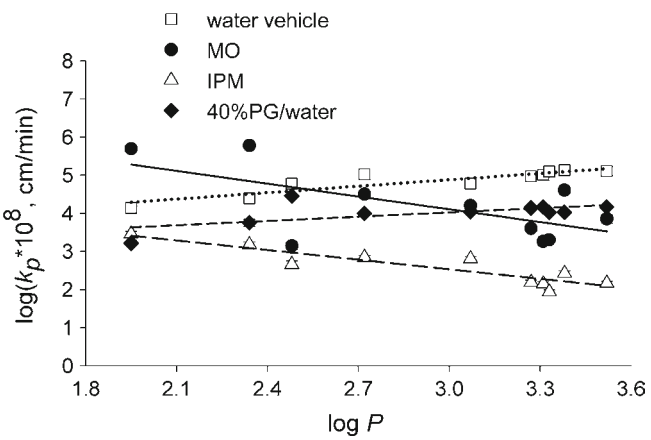

Fig. 3 The plot of log k_p *versus* log *P* (the lines show the linear fit).

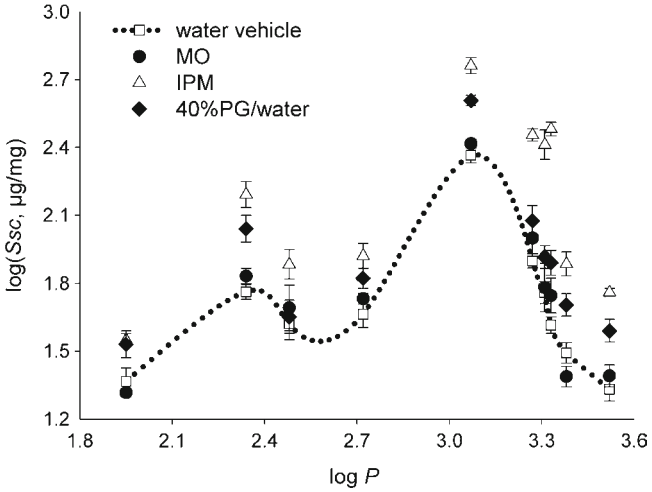

Fig. 4 The plot of log S_{SC} *versus* log *P* (the dashed line included is the interpolation of the data for the water vehicle *versus* log *P* only).

Most studies investigating the role of vehicles in solute transport across membranes have used polymeric membranes. Twist and Zatz (3) showed that methyl paraben had almost identical fluxes for a range of vehicles in which methyl paraben had varying solubilities using polydimethylsiloxane membrane. We showed that hydrocortisone had similar fluxes across silicone membranes for a range of solvents when the solvent did not affect the membrane. However, the hydrocortisone fluxes greatly increased when the solvent caused swelling of the membrane (4). A key concept driving these results is that the same flux will be observed for the same thermodynamic activity of a solute in a vehicle providing the vehicle has not affected the skin or the membrane used. Hence, solute flux should be the same from saturated solutions for a series of "inert" solvents (3,4) or proportional to the thermodynamic activity of the solute

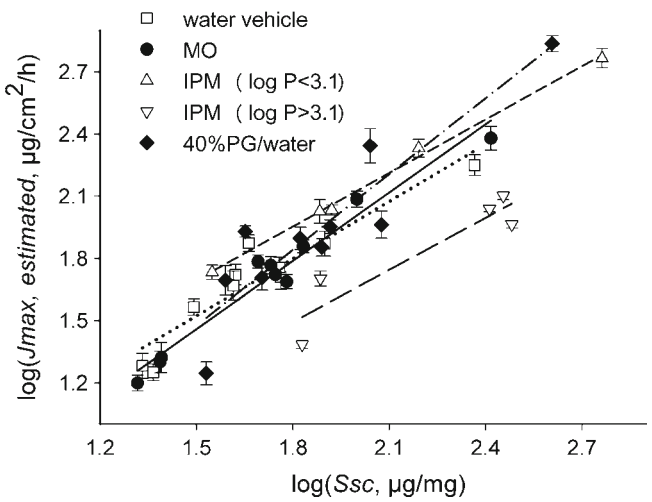

Fig. 5 Linear relationship between log $J_{max,\ estimated}$ and log S_{SC} (dot line: data from water; solid line: data from MO; short dash line: data from IPM, solutes with log $P < 3.1$; long dash line: data from IPM, solutes with log $P > 3.1$; dash-dot line: data from 40%PG/water).

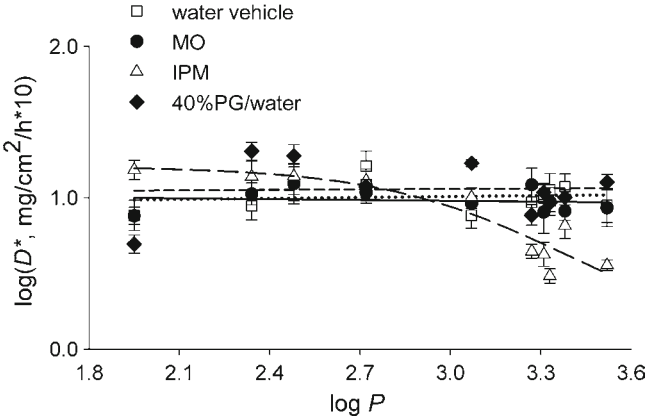

Fig. 6 The plot of log D^* *versus* log *P*.

irrespective of the vehicle, as shown by Barry and his colleagues for the flux of benzyl alcohol through human skin (5) and for the vasoconstriction response to topical corticosteroids (21). Lippold (6) has also shown that the vasoconstrictor activity of steroids was related to their thermodynamic activity. A key issue in comparing MO with water as a vehicle is the extent of hydration of the skin and the species used. Barry's group (22) also showed that the penetration through hairless mouse skin, and not human skin, could increase with the duration of hydration time and this may explain our previous findings of a higher flux for phenol from water than from MO (23). Care must be taken in using phenols as higher concentrations can damage the skin and increase skin penetration (24,25). In this work and in our earlier studies (8,11), concentrations of phenols that do not affect the permeability of human epidermis were used. The observed similar maximum fluxes through human epidermis and solubilities in human stratum corneum for phenols are consistent with MO having an effective occlusive emollient effect (12,14). Variation in skin hydration can greatly affect

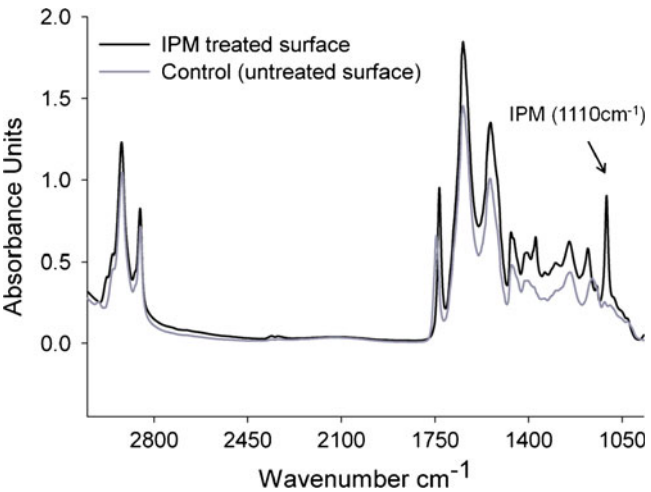

Fig. 7 A typical ATR-FTIR spectrum from human stratum corneum *in vitro* after a 12 h contact with IPM. The C-O stretching absorbance band from IPM is highlighted.

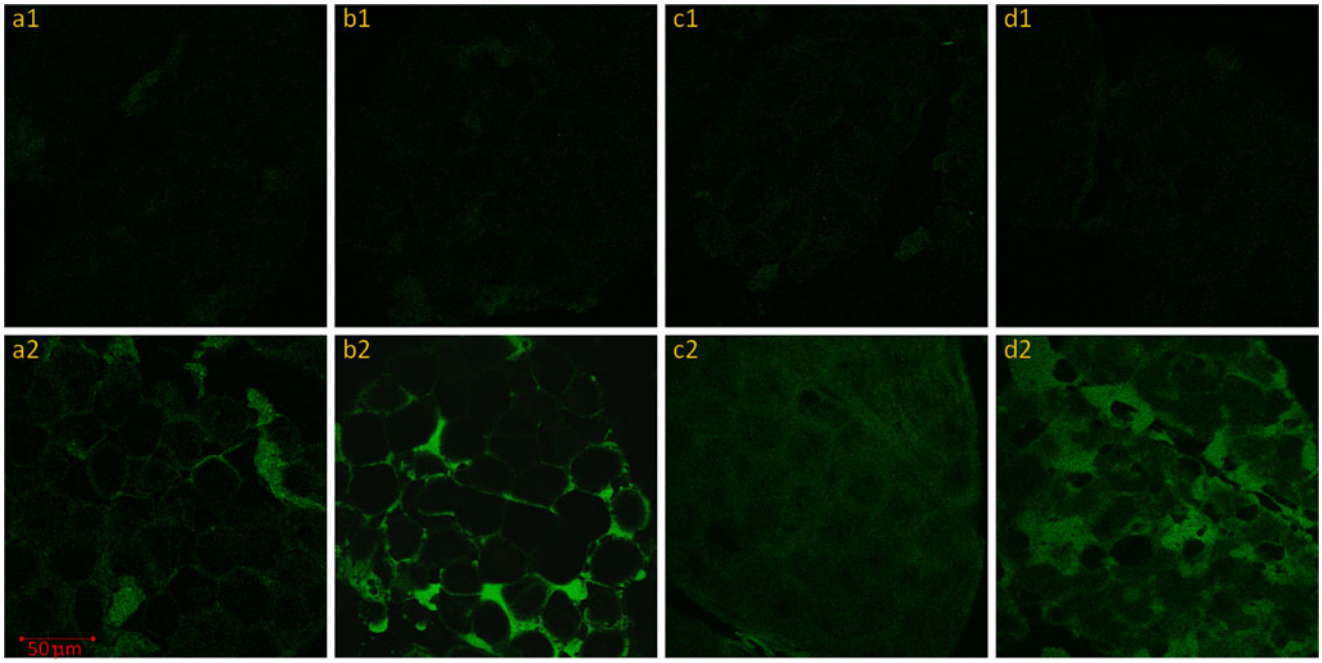

Fig. 8 Multiphoton microscopy images of human stratum corneum (all scans were collected 5 μm below the skin surface. (**a1**–**d1**) Control samples treated by water, 40%PG/water, MO and IPM only; (**a2**–**d2**) saturated solutions of β-naphthol in water, 40%PG/water, MO and IPM treated samples, respectively. Scale bar shows 50 μm).

solute skin penetration as we have shown for a series of phenols through human skin (26).

Our work showing that log K_{SC} and log k_p *versus* log P has positive slopes for polar vehicles (8,11) and negative slopes for lipophilic vehicles (Figs. 2 and 3) are consistent with findings that we (26) and Blank (27) have shown for phenols and alcohols, respectively. The linear relationships between log k_p *versus* log P (Fig. 3) together with D^* being independent of log P (Fig. 6) for these phenols of similar size, for polar solvents and MO, support Potts and Guy's contention that the convex relationships between log k_p and log P for our previous phenol results (24) arise from size differences rather than the diffusion barriers explanation we had advanced at that time.

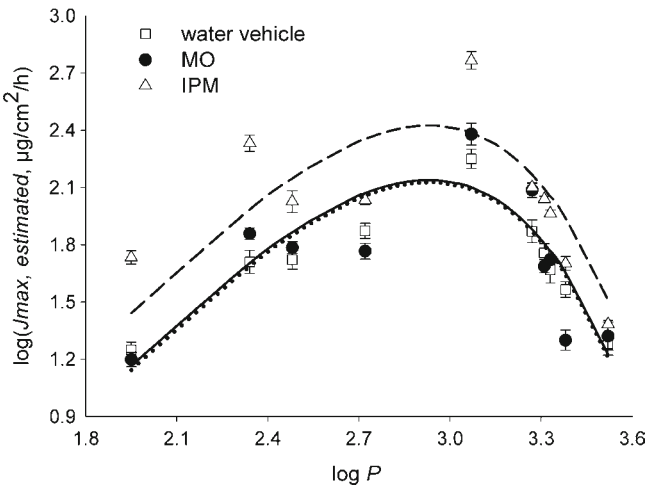

Fig. 9 Bilinear model fits for log $J_{max,\ estimated}$ values from three vehicles *versus* log P (log $J_{max,\ estimated} = -2.1 + 1.7\log P - 21.6\log [10^{-4}(\pm 2.6\cdot 10^{-6})\cdot 10^{\log P} + 1] + S_f$, S_f=0 for water vehicle, S_f =0.3 ±0.1 (SD) for IPM, S_f =0.0 ± 0.1(SD) for MO, respectively).

A unique finding in this work is that IPM showed profiles for log $J_{\max,estimated}$, log S_{SC} and log D^* *versus* log P for the various phenols that differed from what was found for MO and the polar solvents. The differences are almost certainly due to the presence of IPM in the stratum corneum as we showed that three times as much IPM than MO was taken up into the stratum corneum and our ATR-FTIR data (Fig. 7) suggests IPM may diffuse and stay in the deeper layers of the stratum corneum. A high affinity of IPM to the stratum corneum can be attributed to it having a similar solubility parameter [$(8.03\ \text{cal cc}^{-1})^{1/2}$] to skin [$(9.8\ \text{cal cc}^{-1})^{1/2}$] (28–30). Indeed, it has been suggested that IPM can integrate into the lipophilic regions of stratum corneum lipid matrix (31). Such an integration could lead to a disruption of the organised lipid bilayer lamellae that constitute the intercellular region in the stratum corneum and a higher D^* for the more polar phenols (log P<2.8) as shown in Fig. 6. Several FTIR (30,32,33) and differential scanning calorimetry studies (34) have suggested that IPM could increase the lipid fluidity in the lipid components of the stratum corneum. Together with the IPM induced enhancement of all phenols S_{SC} (Fig. 4), the resultant increased D^* results in an enhanced maximum transepidermal flux for polar phenols (Fig. 1).

A less enhanced maximum flux for the more lipophilic phenols from IPM than that for polar phenols (Fig. 1) was

unexpected. However, Pillai and Panchagnula (32) have suggested that IPM will have a minimal effect on the skin barrier and Brinkmann and Muller-Goymann (35) suggested an IPM uptake into the stratum corneum would lead to densely packed lipid bilayers. An analysis of the determinants of maximum flux suggests that whilst IPM increases S_{SC} for the lipophilic phenols, this is counterbalanced by a reduced D^* for these more lipophilic phenols. One explanation for the IPM effect is that the enhanced S_{SC} of phenols (Fig. 4) arises from significant partitioning into immobile pools of IPM in the stratum corneum. Indeed, Liu *et al.* (36) have argued that IPM is largely retained in the stratum corneum and unlikely to traverse the skin. The effect of these pools on diffusion is most likely to become evident only for the more lipophilic phenols as these have a high affinity for IPM (Table II). The effective diffusivity in this case $D^*_{effective}$ would be given by $D^*/(1+K_{IPM,\ pool})$ (37) where $K_{IPM,\ pool}$ is the partition coefficient between the IPM lipid pool and the usual path for these phenols diffusion in the stratum corneum. Accordingly, it will appear that $D^*_{effective}$ has decreased. It is possible that the IPM pools could be in the stratum corneum lipids as we have speculated for certain oils (38). It is also possible that some IPM has entered the corneocytes and formed a lipid pool there. Indeed, our multiphoton microscopy results (Fig. 8) are consistent with the findings of Winckle *et al.* (20), who showed a more ubiquitous distribution for the fluorescence of the lipophilic phenol, β-naphthol, in the stratum corneum from the IPM vehicle. The process may be further complicated by possible self-association of these lipophilic solutes at high concentrations as we have found for octyl salicylate (39). Obviously, further studies are needed to better understand the reasons for the IPM effects on phenolic solute human epidermal penetration and diffusion relationships found here.

Riviere and Brooks (40) have recently advocated the use of a mixture factor to predict the effects of individual vehicles on the skin penetration of solutes. We applied this concept in Fig. 9, using a bilinear model to describe the relationship between log $J_{\max,estimated}$ *versus* log P and a solvent factor (S_f), normalised to a S_f of zero for the water vehicle, to adjust for the effects of different vehicles in this study. It is evident that the model provides only an approximate description of all of the experimental data and yields S_f values of 0.3 ± 0.1 (SD) for IPM and 0.0 ± 0.1 (SD) for MO vehicle (Fig. 9).

CONCLUSION

This study has shown that the human transepidermal maximum fluxes, solubility in the stratum corneum and diffusivity per unit path length for phenols of similar size but different lipophilicity from a MO vehicle are similar to findings we previously reported for a water vehicle. In contrast, an IPM vehicle leads to enhanced maximum fluxes and diffusivity per unit path length for the polar phenols but with maximum fluxes similar to a water vehicle for the more lipophilic phenols. It appears that these lipophilic phenols have an enhanced solubility in the stratum corneum that is counterbalanced by a decreased diffusivity per unit path length.

ACKNOWLEDGMENTS AND DISCLOSURES

This work was supported by the National Health and Medical Research Council of Australia.

REFERENCES

1. Barry BW, Harrison SM, Dugard PH. Correlation of thermodynamic activity and vapour diffusion through human skin for the model compound, benzyl alcohol. J Pharm Pharmacol. 1985;37(2):84–90.
2. Rosado C, Cross SE, Pugh WJ, Roberts MS, Hadgraft J. Effect of vehicle pretreatment on the flux, retention, and diffusion of topically applied penetrants *in vitro*. Pharm Res. 2003;20(9):1502–7.
3. Twist JN, Zatz JL. Influence of solvents on paraben permeation through idealized skin model membranes. J Soc Cosmet Chem. 1986;37:429–44.
4. Cross SE, Pugh WJ, Hadgraft J, Roberts MS. Probing the effect of vehicles on topical delivery: understanding the basic relationship between solvent and solute penetration using silicone membranes. Pharm Res. 2001;18(7):999–1005.
5. Barry BW, Harrison SM, Dugard PH. Vapour and liquid diffusion of model penetrants through human skin; correlation with thermodynamic activity. J Pharm Pharmacol. 1985;37(4):226–36.
6. Lippold BC. How to optimize drug penetration through the skin. Pharm Acta Helv. 1992;67(11):294–300.
7. Magnusson BM, Anissimov YG, Cross SE, Roberts MS. Molecular size as the main determinant of solute maximum flux across the skin. J Invest Dermatol. 2004;122(4):993–9.
8. Zhang Q, Grice JE, Li P, Jepps OG, Wang GJ, Roberts MS. Skin solubility determines maximum transepidermal flux for similar size molecules. Pharm Res. 2009;26(8):1974–85.
9. Cross SE, Anderson C, Roberts MS. Topical penetration of commercial salicylate esters and salts using human isolated skin and clinical microdialysis studies. Br J Clin Pharmacol. 1998;46(1):29–35.
10. Cross SE, Roberts MS. The effect of occlusion on epidermal penetration of parabens from a commercial allergy test ointment, acetone and ethanol vehicles. J Invest Dermatol. 2000;115(5):914–8.
11. Zhang Q, Li P, Roberts MS. Maximum transepidermal flux for similar size phenolic compounds is enhanced by solvent uptake into the skin. J Control Release. 2011;154(1):50–7.
12. Stamatas GN, de Sterke J, Hauser M, von Stetten O, van der Pol A. Lipid uptake and skin occlusion following topical application of oils on adult and infant skin. J Dermatol Sci. 2008;50(2):135–42.
13. Blanken R, van Vilsteren MJ, Tupker RA, Coenraads PJ. Effect of mineral oil and linoleic-acid-containing emulsions on the skin vapour loss of sodium-lauryl-sulphate-induced irritant skin reactions. Contact Dermatitis. 1989;20(2):93–7.
14. Parente ME, Gambaro A, Solana G. Study of sensory properties of emollients used in cosmetics and their correlation with physicochemical properties. J Cosmet Sci. 2005;56(3):175–82.

15. Campbell RL, Bruce RD. Comparative dermatotoxicology. I Direct comparison of rabbit and human primary skin irritation responses to isopropylmyristate. Toxicol Appl Pharmacol. 1981;59 (3):555–63.
16. Suh H, Jun HW. Effectiveness and mode of action of isopropyl myristate as a permeation enhancer for naproxen through shed snake skin. J Pharm Pharmacol. 1996;48(8):812–6.
17. Kligman AM, Christophers E. Preparation of Isolated Sheets of Human Stratum Corneum. Arch Dermatol. 1963;88:702–5.
18. Roberts MS, Triggs EJ, Anderson RA. Permeability of solutes through biological membranes measured by a desorption technique. Nature. 1975;257(5523):225–7.
19. Anderson RA, Triggs EJ, Roberts MS. The percutaneous absorption of phenolic compounds. 3. Evaluation of permeability through human stratum corneum using a desorption technique. Aust J Pharm Sci. 1976;5(4):107–10.
20. Winckle G, Anissimov YG, Cross SE, Wise G, Roberts MS. An integrated pharmacokinetic and imaging evaluation of vehicle effects on solute human epidermal flux and, retention characteristics. Pharm Res. 2008;25(1):158–66.
21. Bennett SL, Barry BW, Woodford R. Optimization of bioavailability of topical steroids: non-occluded penetration enhancers under thermodynamic control. J Pharm Pharmacol. 1985;37 (5):298–304.
22. Bond JR, Barry BW. Limitations of hairless mouse skin as a model for *in vitro* permeation studies through human skin: hydration damage. J Invest Dermatol. 1988;90(4):486–9.
23. Roberts MS, Anderson RA. The percutaneous absorption of phenolic compounds: the effect of vehicles on the penetration of phenol. J Pharm Pharmacol. 1975;27(8):599–605.
24. Roberts MS, Anderson RA, Swarbrick J. Permeability of human epidermis to phenolic compounds. J Pharm Pharmacol. 1977;29 (11):677–83.
25. Behl CR, Linn EE, Flynn GL, Pierson CL, Higuchi WI, Ho NF. Permeation of skin and eschar by antiseptics I: baseline studies with phenol. J Pharm Sci. 1983;72(4):391–7.
26. Roberts MS. Structure-permeability considerations in percutaneous absorption. In: Scott RC, Guy RH, Hadgraft J, Boddé HE, editors. Prediction of percutaneous penetration. London: IBC Technical Services; 1991. p. 210–28.
27. Blank IH. Penetration of low-molecular-weight alcohols into skin. I. effect of concentration of alcohol and type of vehicle. J Invest Dermatol. 1964;43:415–20.
28. Vaughan CD. Using solubility parameters in cosmetic formulation. J Soc Cosmet Chem. 1985;36:319–33.
29. Liron Z, Cohen S. Percutaneous absorption of alkanoic acids II: Application of regular solution theory. J Pharm Sci. 1984;73 (4):538–42.
30. Panchagnula R, Desu H, Jain A, Khandavilli S. Feasibility studies of dermal delivery of paclitaxel with binary combinations of ethanol and isopropyl myristate: role of solubility, partitioning and lipid bilayer perturbation. Farmaco. 2005;60(11–12):894–9.
31. Brinkmann I, Muller-Goymann CC. An attempt to clarify the influence of glycerol, propylene glycol, isopropyl myristate and a combination of propylene glycol and isopropyl myristate on human stratum corneum. Pharmazie. 2005;60(3):215–20.
32. Pillai O, Nair V, Panchagnula R. Transdermal iontophoresis of insulin: IV Influence of chemical enhancers. Int J Pharm. 2004;269 (1):109–20.
33. Furuishi T, Fukami T, Suzuki T, Takayama K, Tomono K. Synergistic effect of isopropyl myristate and glyceryl monocaprylate on the skin permeation of pentazocine. Biol Pharm Bull. 2010;33(2):294–300.
34. Leopold CS, Lippold BC. An attempt to clarify the mechanism of the penetration enhancing effects of lipophilic vehicles with differential scanning calorimetry (DSC). J Pharm Pharmacol. 1995;47 (4):276–81.
35. Brinkmann I, Muller-Goymann CC. Role of isopropyl myristate, isopropyl alcohol and a combination of both in hydrocortisone permeation across the human stratum corneum. Skin Pharmacol Appl Skin Physiol. 2003;16(6):393–404.
36. Liu P, Cettina M, Wong J. Effects of isopropanol-isopropyl myristate binary enhancers on *in vitro* transport of estradiol in human epidermis: a mechanistic evaluation. J Pharm Sci. 2009;98(2):565–72.
37. Roberts MS, Cross SE, Pellett MA. Skin transport. In: Walters KA, editor. Dermatological and transdermal formulations. New York: Marcel Dekker; 2002. p. 89–195.
38. Menon GK, Lee SH, Roberts MS. Ultrastructural effects of some solvents and vehicles on the stratum corneum and other skin components: Evidence for an "extended mosaic-partitioning model of the skin barrier". In: Roberts MS, Walters KA, editors. Dermal absorption and toxicity assessment. New York: Blackwell Publishing; 1998. p. 727–51.
39. Jiang R, Roberts MS, Prankerd RJ, Benson HA. Percutaneous absorption of sunscreen agents from liquid paraffin: self-association of octyl salicylate and effects on skin flux. J Pharm Sci. 1997;86 (7):791–6.
40. Riviere JE, Brooks JD. Predicting skin permeability from complex chemical mixtures. Toxicol Appl Pharmacol. 2005;208(2):99–110.